

RePPL: Recalibrating Perplexity by Uncertainty in Semantic Propagation and Language Generation for Explainable QA Hallucination Detection

Yiming Huang^{1*}, Junyan Zhang^{1*}, Zihao Wang², Biquan Bie³, Yunzhong Qiu⁴,
Yi R. (May) Fung², Xinlei He^{1†}

¹The Hong Kong University of Science and Technology, Guangzhou,

²The Hong Kong University of Science and Technology,

³Independent Researcher, ⁴Tsinghua University

Abstract

Large Language Models (LLMs) have become powerful, but hallucinations remain a vital obstacle to their trustworthy use. Previous works improved the capability of hallucination detection by measuring uncertainty. But they can not explain the provenance behind why hallucinations occur, particularly in identifying which part of the inputs tends to trigger hallucinations. Recent works on the prompt attack indicate that uncertainty exists in semantic propagation, where attention mechanisms gradually fuse local token information into high-level semantics across layers. Meanwhile, uncertainty also emerges in language generation, due to its probability-based selection of high-level semantics for sampled generations. Based on that, we propose **RePPL** to recalibrate uncertainty measurement by these two aspects, which dispatches explainable uncertainty scores to each token and aggregates in Perplexity-style Log-Average form as total score. Experiments show that our method achieves the best comprehensive detection performance across various QA datasets on advanced models (average AUC of 0.833), and it is capable of producing token-level uncertainty scores as explanations for the hallucination. Leveraging these scores, we find the chaotic uncertainty pattern of hallucination (more uncertainty-inducing tokens are less important) and showcase its promising usage.

Introduction

Since the milestone work ChatGPT (OpenAI 2023) has revolutionized the fields of Language Generation, powerful Large Language Models (LLMs) are constantly updating and continuously shaping the text-driven automation in everyday applications like chatbots, document summarizers, and AI search engines. Despite these successes, one of the fatal shortcomings of LLMs is hallucination, i.e., factually incorrect or contextually inconsistent outputs. Due to the urgent demand for trustworthiness in these LLM-based applications, detecting hallucination and figuring out how LLMs hallucinate is crucial to building robust AI systems.

To tackle question answering (QA) hallucination in LLM, prior works (Ren et al. 2023; Liu et al. 2020; Lin, Hilton, and Evans 2022; Malinin and Gales 2021; Farquhar et al. 2024; Chen et al. 2024) identify the uncertainty of generations as the key point. These methods can be divided into two groups:

*These authors contributed equally.

†Correspondence: xinleihe@hkust-gz.edu.cn

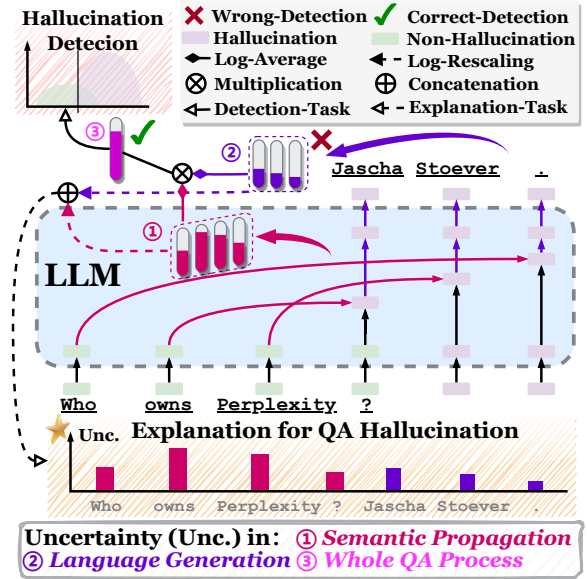


Figure 1: Illustration of our motivation. The LLM (Llama-3.1-8B-Instruct) generates a hallucinated answer “Jascha Stoever” to the question “Who owns Perplexity?”, with high-confidence (low-uncertainty) logits. This makes the detection hard for existing methods using logits. While our method judges it correctly with the explanation, by balancing uncertainty in semantic propagation and language generation.

logits-based and sampling-based methods. The logits-based methods (Ren et al. 2023; Liu et al. 2020; Lin, Hilton, and Evans 2022) utilize the confidence of each token’s generation to accumulate uncertainty, while the sampling-based (Malinin and Gales 2021; Farquhar et al. 2024; Chen et al. 2024) methods measure the discrepancy between sampled generations as uncertainty. However, these detection methods cannot explain why LLMs hallucinate and which part of the inputs mainly triggers the hallucination.

Our motivation stems from two observations. Firstly, recent works (Xu et al. 2024; Liu et al. 2024b) about LLMs’ prompt attack applied to different parts of inputs can easily trigger various LLMs’ untrustworthy output, including hallucinations. This suggests that uncertainty arises in semantic

propagation, where attention gradually fuses local token information into high-level semantics across layers. Secondly, the confidences of generations represented by logits often vary between different tokens and different generations. It implies that probability-based token generation selectively discards the remaining high-level semantics, bringing uncertainty in language generation. As Figure 1 shows, we aim to combine these two aspects for better hallucination detection.

From this viewpoint, we propose **RePPL** to recalibrate uncertainty by these two aspects with **Perplexity**-style aggregation. For the intrinsic semantic propagation, we utilize the attribution-based explainability method (Abnar and Zuidema 2020; Chefer, Gur, and Wolf 2021) to compute token-level uncertainty (inverse of confidence) by measuring token attribution discrepancies across sampled generations. For the extrinsic language generation, we normalize token confidence by the average generation length of sampling to make the confidence more distinct. As Figure 1 depicts, uncertainty (or confidence) scores correspond to each token as the explanation in these two aspects. And we use **Perplexity**-style (Ren et al. 2023) aggregation that firstly rescales confidence into log form, then averages them all. We name these two total scores as **InnerPPL** and **OuterPPL**. Through multiplying them, we derive the recalibrated hallucination score **RePPL** with hierarchical distinctness from the above two aspects. Experiments show that our method comprehensively outperforms baselines across QA datasets, achieving an average AUC of 0.833. It also faithfully explains hallucination by highlighting the uncertainty-inducing tokens. Meanwhile, we find the chaotic uncertainty pattern of hallucination through correlation between these uncertainty scores and attribution-based importance scores, where more uncertainty-inducing tokens that mainly trigger hallucinations are less important.

To summarize, the contribution of this work can be concluded as the following threefold:

1. We address the novel view of balancing uncertainty in semantic propagation and language generation, which brings recalibrated uncertainty with token-correspondence and hierarchical distinctness to propose our innovative hallucination detection score **RePPL** with explainability.
2. Our proposed **RePPL** achieves the leading performance in hallucination detection tasks across various datasets and models. And it is also robust under different hyperparameter settings and sampling options.
3. **RePPL**'s uncertainty scores are pioneering in explaining the hallucination triggered by both input prompts and output contents. It provides a faithful token-level explanation by indicating uncertainty-inducing tokens and serves as a useful statistical signal for analyzing attention disorder and the hallucination pattern of chaotic uncertainty.

Related Works and Background

Uncertainty in Hallucination Detection

Uncertainty measurement (Fakour, Mosleh, and Ramezani 2024; Sun, Chen, and Carin 2017) is a classic research topic in the wide machine learning domain. It is highly related to out-of-distribution detection, which is inherently correlated

to hallucination detection (Zhang et al. 2024; Ma et al. 2025). For non-parameterized methods, uncertainty-based hallucination detection can be mainly sorted into two kinds. The first is the logits-based, like widely used **Perplexity** (Ren et al. 2023) and typical **Verbalize** (Lin, Hilton, and Evans 2022) a.k.a. $P(\text{True})$, these methods exert confidence within logits to figure up uncertainty in a single generation. The second is the sampling-based, for instance, **Semantic Entropy** (Farquhar et al. 2024) and **EigenScore** (Chen et al. 2024). These methods take the discrepancy between different generations as uncertainty. Despite the effectiveness of these methods, they only pay attention to uncertainty in generation. It hinders them from exploiting the process of how input transforms into output, namely the semantic propagation, for better performance and potential explainability.

For parameterized methods, we also notice the powerful probe-based method (Orgad et al. 2024; Liu et al. 2024a; Wang et al. 2024). But they have two main shortcomings: 1. Regarding binary classification, they need adjustments and extra implementations with task-specific losses or hyperparameters for peak performance on abundant training data. 2. As for the hallucination degree comparator, they are unsuitable as a zero-shot hallucination degree indicator for scenarios like tracing and comparing hallucination risks of the LLM in the pretraining stage. We hence consider them more cost-effective for target LLMs and additionally compare them in Appendix E, F, and G with our method.

Attribution Explanation

In the explainable AI (XAI) domain, attribution is an enduringly appealing topic as it indicates the salient part of the model's inputs to the model's prediction. For model-specific ones, **Rollout** (Abnar and Zuidema 2020), **GenAtt** (Chefer, Gur, and Wolf 2021), and **AttnLRP** (Achtibat et al. 2024) improve the attribution ability by utilizing attention maps among different layers of transformers. For model-agnostic ones, like **LIME**-style (Ribeiro, Singh, and Guestrin 2016) and **Shapley**-value-based (Lundberg and Lee 2017; Lundberg, Erion, and Lee 2018), they need sufficient input perturbation for measuring the importance of absent tokens. Because model-specific methods need expensive gradients and model-agnostic methods need too many throughputs to guarantee their precision, they are intractable in explaining real-time hallucination detection. Therefore, we adopt simple maximum, average, and **Rollout** to pool attention maps as attribution across layers and heads. These attribution methods commonly generate an attribution map, and the row of this map represents the token-to-token contribution importance (scores). At the instance level, we attribute the uncertainty score expressing token-wise propensity to induce hallucinations rather than the importance score by the above methods, as the explanation of hallucination. At the macro-level, it is also useful to explore the underlying factors of the hallucination pattern, like prior works (Zhang et al. 2025; Ferrando et al. 2025; Yu et al. 2024; Orgad et al. 2024).

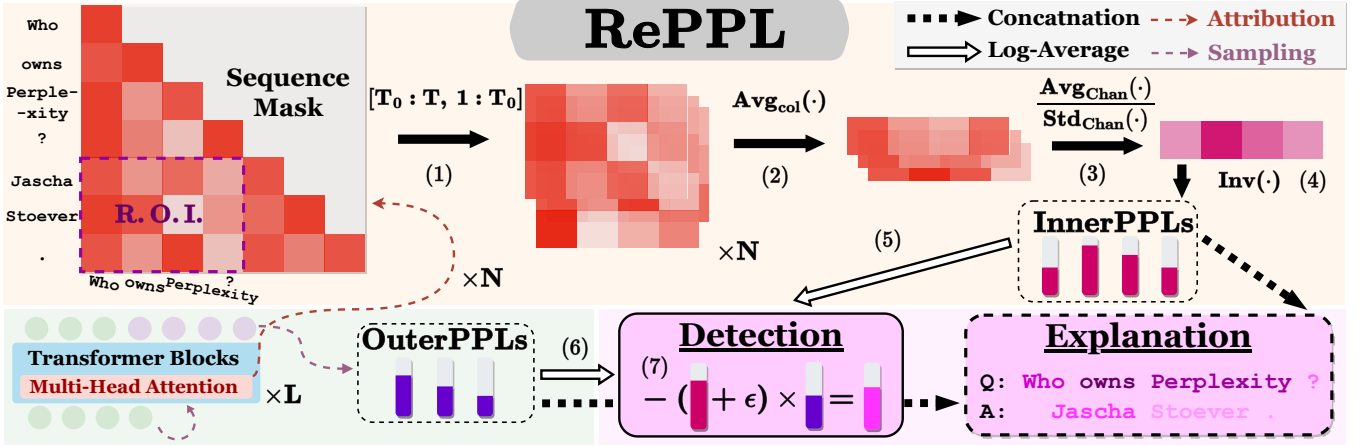


Figure 2: Detailed illustration of **RePPL** computing process. (1) ~ (7) correspond to the same equations in paper. ‘InnerPPLs’ and ‘OuterPPLs’ with plural form to indicate token-wise confidence scores.

Methodologies

Attention-based Attribution

As discussed above, we choose the following three attention pooling strategies. The first is maximum pooling, abbreviated as **MaxPool**. Given attention maps of t tokens $\mathbf{A}^{(l)} \in \mathbb{R}^{h \times t \times t}$ across different attention heads h of attention in layer l in L layers transformer-based LLM. We take the final attribution $\mathbf{R} \in \mathbb{R}^{t \times t}$ as:

$$\mathbf{R} = \text{MaxPool}(\mathcal{A}) = \text{Max}_l(\text{Max}_h(\mathcal{A})),$$

here, $\mathcal{A} = [\mathbf{A}_1, \mathbf{A}_2, \dots, \mathbf{A}_L]$ is the attention maps concatenation along the layer dimension and Max_d is the maximum selection among values along d dimension. Similarly, the average pooling **AvgPool** is (Avg_d is the average operation):

$$\mathbf{R} = \text{AvgPool}(\mathcal{A}) = \text{Avg}_l(\text{Avg}_h(\mathcal{A})).$$

As for Rollout (Abnar and Zuidema 2020) pooling **RollPool**, it layer-wisely accumulates relevance from equal single-head attention $\bar{\mathbf{A}}$ as attribution, meanwhile, it also considers the relevance in the residual part. We adopt same enhancement in GenAtt (Chefer, Gur, and Wolf 2021) as follows:

$$\begin{aligned} \mathbf{R}^{(l)} &\leftarrow \mathbf{R}^{(l-1)} + \mathbf{R}^{(l-1)} \cdot \bar{\mathbf{A}}_l, \\ \bar{\mathbf{A}}_l &= \text{Norm}_{\text{row}}(\text{Avg}_h(\mathbf{A}_l^+) - \mathbb{I})/2 + \mathbb{I}/2, \end{aligned}$$

therein, it begin with the initialization $\mathbf{R}^{(0)} := \mathbb{I}$, Norm_{row} is the normalization ($\mathbf{p} = 1$) across horizontal rows of matrix, \mathbb{I} is the identical matrix and we count the $\mathbf{R}^{(L)}$ end up at layer L as the final attribution. In our application context, these attributions prepare the granular token-to-token importance scores for both detailed and explainable semantic propagation measurement, and they are more efficient than others.

Uncertainty Recalibration

Overview. The final uncertainty score is recalibrated by multiplying the inner semantic propagation uncertainty derived from attribution variance across samples, and the outer language generation uncertainty based on a modified aggregation of token-level confidence.

InnerPPL. For inner semantic propagation, providing the abovementioned attribution matrix \mathbf{R} (also row-normalized) after LLM’s inference (detailed in Figure 2), we convert importance to the uncertainty score of each token and aggregate them as the following steps. Firstly, we sample N times from the LLM, which empowers uncertainty to appear between the attribution matrices $\{\mathbf{R}_1, \mathbf{R}_2, \dots, \mathbf{R}_N\}$, $\mathbf{R}_n \in \mathbb{R}^{T_n}$ of different generations, T_n is the total length of input tokens added up with output tokens and T_0 in the length of input tokens. In these attribution matrices, the region of interest (**R.O.I.**) is the columns from the first column to the T_0 column in rows from the T_0 row to the T_n row, because they represent each input token’s semantic contribution in the propagation process of each output token. These regions reflect how the input token propagates its own semantics into high-level semantics, which are selected by generated tokens. That is:

$$\mathcal{R}_{roi} = \{\mathbf{R}_{n, [T_0:T_n, 1:T_0]} | n \in \{1, 2, \dots, N\}\}. \quad (1)$$

Here, $[a : b, c : d]$ is the continuous submatrix selection operation which selects the submatrix of the a -th row to b -th row and c -th column to d -th column of \cdot . Thus, the uncertainty of semantic propagation can be derived by measuring the discrepancy of these regions in different sampling channels. Then, we average different columns across the rows of each attribution submatrix (col refers to columns dimension):

$$\bar{\mathcal{R}}_{roi} = \text{Avg}_{\text{col}}(\mathcal{R}_{roi}) \in \mathbb{R}^{N \times T_0}. \quad (2)$$

These attribution submatrices are condensed into vectors with T_0 length and N sampling channels. They express the average semantic propagation on all generated tokens, which also gets rid of the different generation lengths. To derive uncertainty in sampling channels, we choose the coefficient of variation that is scale-/unit-independent for undistorted uncertainty measurement. That is the following equation (chan refers to channels dimension):

$$\mathbf{r} = \frac{\text{Std}_{\text{chan}}(\bar{\mathcal{R}}_{roi})}{\text{Avg}_{\text{chan}}(\bar{\mathcal{R}}_{roi})}, \quad (3)$$

it directly uses the standard deviation (Std) divided by the average. The coefficient of variation vector \mathbf{r} quantifies the uncertainty of different input tokens. Next, we use the inverse function to transform this coefficient of variation vector to pseudo-confidences similar to logit-based probabilities:

$$\hat{\mathbf{p}} \in [0, 1]^{T_0}, \hat{p}_i = \text{Inv}(r_i) = \frac{1}{1 + r_i^\alpha}. \quad (4)$$

Here, α is the hyperparameter that controls uncertainty scaling. Subsequently, similar to the Perplexity (Ren et al. 2023), we adopt log rescaling and length-as-divisor average of $\hat{\mathbf{p}}$ to calculate the total score in inner side semantic propagation:

$$\text{InnerPPL} = -\frac{1}{T_0} \sum_{i=1}^{T_0} \log(\hat{p}_i). \quad (5)$$

The \log enlarges the significant part of the uncertainty, thus more validly takes it into account for hallucination.

OuterPPL. For the outer part of language generation, given the g -th generated token confidence \mathbf{p}_g and generation length S_g at the greedy decoding stage, we compute the overall generation uncertainty as:

$$\text{OuterPPL} = -\frac{1}{\bar{S}} \sum_{g=1}^{S_g} \log(\mathbf{p}_g), \quad (6)$$

\bar{S} is the average length of N sampled generations. The only difference between our **OuterPPL** and the original PPL is different divisors. The rationale behind this divisor is that we observe (as shown in Figure 3) that the generation length of the greedy decoding is basically shorter than sampling generations when LLM is certain. On the contrary, if LLM tends to hallucinate, the greedy path is roughly equal to most sampling paths. Thus, this divisor plays the role of a reward or penalty factor to make outer uncertainty more discriminative.

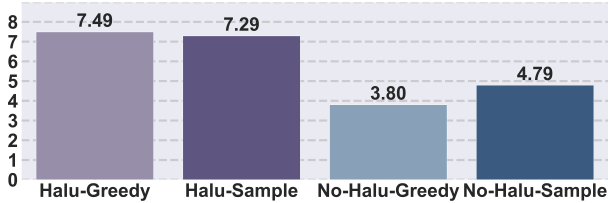


Figure 3: Length of greedy (‘Greedy’) outputs and average length of sampled generations (‘Sample’) of 1000 examples in TriviaQA. ‘Halu’ is hallucinated ones, and ‘No-Halu’ is the not hallucinated ones.

RePPL. Finally, our **RePPL** is derived from the multiplication of these two scores, which means recalibration of uncertainty from the two aspects. It is:

$$\text{RePPL} = -(\text{InnerPPL} + \epsilon) \times \text{OuterPPL}. \quad (7)$$

In the above equation, ϵ is the preset bias term, which is the default value to express correct uncertainty in case **InnerPPL** is 0 but **OuterPPL** is still large. In general, we

choose $\frac{1}{10} \sim \frac{1}{5}$ of average **InnerPPL** value for ϵ . Since the multiplication form of our hallucination score comprehensively considers uncertainty in semantic propagation and language generation, it is capable of hierarchical division when **InnerPPL** is large but **OuterPPL** is small, or vice versa. This trait equipped our method more layered distinctness for better detection. As for the uncertainty (or confidence) scores that granularly express token-wise contribution to hallucination, we collect them from the above computing process as an explanation of hallucination. These token-by-token scores attribute uncertainty rather than importance, thus figure out which input tokens trigger hallucination and which output tokens are more likely to be the hallucination.

Evaluation

Experimental Setup

Datasets. Question answering (QA) is the most common scenario for LLM-based applications. We choose four widely used QA datasets to evaluate our proposed hallucination score. Two of them are closed-book QA datasets, i.e., TriviaQA (Joshi et al. 2017) and Natural Questions (NQ) (Kwiatkowski et al. 2019). TriviaQA is a dataset that assembles trivia knowledge questions with precise answers, we select 9960 QA pairs in the validation split of *rc.noncontext* subset after deduplication. NQ is a dataset composed of Google search-based QA pairs. We choose the 3610 QA pairs in the validation split for evaluation, same as Chen et al. (2024). The other two are open-book QA datasets, i.e., CoQA (Reddy, Chen, and Manning 2019) and SQuAD (Rajpurkar et al. 2016). CoQA is a dataset about conversational QA, we utilize the development split of CoQA with 7983 QA pairs for our experiment. As for SQuAD, it is a reading comprehension dataset, and we take the development-v2.0 split with 5928 QA pairs (with filter condition *is_impossible=True*). All of the above subset selections are the same as prior work of Chen et al. (2024).

Target Models. We choose three representative open-source models Llama-3.1-8B-Instruct (Grattafiori et al. 2024), Qwen2.5-7B-Instruct, and Qwen2.5-14B-Instruct (Yang et al. 2024) for experiments. Currently, they are widely used in diversified applications, and they are popular in various leadboards. Since they are high-performance instruction-finetuned models, we believe their error can represent hallucination issues well in general application scenarios.

Inference Settings. On account of the instruction finetuned models, we equip them with a normal chat template described in Appendix B. For sampling-based methods, including ours, in line with prior works (Farquhar et al. 2024; Chen et al. 2024), we set the number of sampled generations $N = 10$, temperature $\mathcal{T} = 1.0$, sampling hyperparameters Top-K = 50 and Top-P = 0.99 to guarantee the randomness needed by these methods. These inference settings are both fair for comparison and practical for application.

Correctness Measure. Consistent with previous work (Chen et al. 2024), we take the output in greedy decoding as LLM’s canonical response to judge whether it is hallucinated. We follow Du, Xiao, and Li (2024)

Table 1: Evaluation results of different methods on various datasets using AUC, accuracy at threshold of max G-Mean (Acc), and Spearman Correlation (Corr) metrics. Embedding similarity is the correctness measure. We also present performance on the 4 datasets’ merge in the “ALL” columns. The highest values are highlighted in bold, and all values are in percentages.

Models	Datasets Methods	CoQA				TriviaQA				NQ				SQuAD				ALL			
		AUC	Acc	Corr	PRR																
LLaMA-3.1-8B-Instruct	Perplexity	66.6	61.7	30.0	41.7	78.2	71.1	51.0	64.3	77.5	67.5	38.9	46.1	67.4	64.9	31.1	31.3	73.9	67.5	43.8	52.8
	Energy	64.4	59.6	26.5	39.2	67.6	62.6	33.7	42.7	66.3	65.3	26.2	28.3	69.4	64.1	33.4	46.5	69.1	63.4	35.8	48.3
	P(True)	64.0	60.2	25.8	35.1	75.8	69.6	48.7	63.0	69.1	67.0	33.2	38.6	64.4	60.4	25.7	39.7	71.5	65.8	40.9	53.0
	LNPE	72.1	65.7	39.9	50.3	80.2	73.0	55.2	67.6	78.1	68.1	42.8	48.4	69.7	67.2	35.1	34.4	76.8	70.1	49.5	58.5
	Semantic Entropy	74.5	70.6	43.2	54.3	73.6	69.4	43.9	55.9	67.9	69.0	24.3	30.1	66.7	68.6	31.1	39.8	73.9	70.4	44.0	54.0
	EigenScore	77.2	70.6	49.3	62.8	80.5	74.3	55.3	67.7	74.9	71.6	42.4	46.8	76.8	70.9	47.4	61.1	78.2	71.8	51.8	63.7
	AttnScore	75.0	69.4	45.0	48.7	76.0	69.2	44.4	50.0	67.9	62.0	26.6	28.1	64.5	61.7	26.3	30.3	62.6	60.2	21.8	31.2
	RePPL (Ours)	85.2	77.4	61.8	70.7	86.0	78.6	63.2	73.9	79.3	69.9	47.4	51.9	76.0	71.7	45.1	40.6	83.6	76.3	60.0	66.4
Qwen-2.5-7B-Instruct	Perplexity	74.9	71.7	43.3	58.0	83.6	75.9	60.5	71.4	76.8	73.3	39.0	42.4	75.5	69.8	43.5	52.3	80.6	74.3	55.3	65.5
	Energy	53.0	51.8	9.7	17.1	76.3	69.3	50.9	58.6	64.8	57.1	35.6	33.8	59.1	57.7	14.3	19.9	66.1	61.0	33.8	39.4
	P(True)	54.7	53.3	10.3	11.1	79.7	74.3	55.2	65.8	67.5	68.8	22.3	27.6	56.8	57.0	12.3	13.7	70.6	65.3	39.8	46.2
	LNPE	76.8	71.9	46.8	58.8	83.6	76.1	61.2	72.7	77.4	69.1	42.4	42.8	76.1	70.5	44.6	52.7	81.2	74.3	56.9	66.3
	Semantic Entropy	71.3	69.2	39.3	42.6	76.7	76.2	48.3	57.6	72.1	76.9	24.5	28.8	60.8	54.6	19.7	25.0	74.5	72.8	46.0	50.5
	EigenScore	83.0	76.2	58.4	61.3	82.5	75.2	60.2	66.4	79.5	69.7	49.2	47.1	77.3	73.4	46.9	54.1	82.5	75.2	59.8	65.0
	AttnScore	70.7	65.0	34.8	44.1	60.4	57.3	18.6	18.1	63.6	58.7	12.1	12.0	69.9	65.8	35.2	43.0	57.9	62.0	16.1	27.4
	RePPL (Ours)	83.5	77.0	58.4	67.2	84.6	76.3	62.4	73.3	80.0	73.6	45.8	46.5	78.1	71.9	47.8	54.9	83.7	75.9	60.9	68.9
Qwen-2.5-14B-Instruct	Perplexity	74.5	73.6	39.2	43.8	81.4	75.3	56.4	67.1	76.7	70.7	44.2	46.6	75.7	71.5	45.2	48.6	78.0	73.4	49.4	56.3
	Energy	51.3	48.9	18.3	18.1	62.5	58.6	26.5	29.4	58.0	56.8	28.9	29.0	60.8	58.6	18.4	21.8	52.8	50.2	11.4	14.0
	P(True)	58.9	54.4	20.9	22.1	70.1	68.1	41.7	42.2	63.8	66.6	23.9	22.9	53.2	52.9	8.3	0.1	60.0	57.4	23.3	19.4
	LNPE	76.1	75.8	41.3	46.8	82.4	75.5	58.6	69.3	77.2	72.2	46.8	49.5	76.9	71.4	47.4	51.1	79.1	74.2	51.4	57.9
	Semantic Entropy	66.2	53.6	27.9	22.4	73.9	72.9	47.2	49.6	71.7	71.4	31.9	34.1	63.2	59.7	26.1	24.0	69.3	64.1	37.7	34.7
	EigenScore	82.5	72.2	49.7	49.8	81.8	75.5	59.1	65.1	77.7	70.8	51.7	46.4	80.4	73.0	53.5	54.0	81.6	73.2	56.7	56.4
	AttnScore	51.9	51.9	7.6	8.6	64.5	61.0	27.5	30.6	64.5	59.4	25.1	20.6	54.5	53.9	9.3	1.4	64.4	64.1	24.2	30.7
	RePPL (Ours)	79.7	76.6	43.0	47.9	84.8	76.8	62.2	71.9	80.0	71.7	51.4	50.1	81.3	74.4	54.7	56.8	82.5	75.7	56.0	60.4

and Chen et al. (2024) work to use embedding similarity as a correctness measure for ground truth labeling. The sentence embedding of the LLM’s response and the standard answer of the QA pairs are extracted by the model all-MiniLM-L6-v2 (Reimers and Gurevych 2019). We treat embedding similarity between the LLM’s response and the standard answers lower than 0.9 as hallucination. Besides that, we also supplement the experiment using ROUGE-L (f-measure) (Lin 2004) and LLM-as-a-judge (using DeepSeek-R1-250528) (Li et al. 2024) as the correctness measure in Appendix E and G.

Evaluation Metrics. To comprehensively evaluate the performance of hallucination detection scores, similar to Chen et al. (2024), we examine them by three metrics. The first is the widely acknowledged area under the receiver operator characteristic curve (AUC). The second is accuracy (Acc) at the classification threshold of deriving the maximum **G-Mean** value. **G-Mean** is defined as $\text{G-Mean} = \sqrt{\text{TPR} \times (1 - \text{FPR})}$, where TPR is true positive rate and FPR is false positive rate. This accuracy is well recognized when evaluating classification performance in imbalanced situations. Thirdly, we select Spearman Correlation (Corr) to fairly compare the correlation between hallucination scores and ground truth labels. Lastly, we also use the PRR metric in recent work of Vashurin et al. (2025), which is a well-established metric for evaluating uncertainty quantification methods. For these metrics, higher scores indicate better performance. These metrics are detailed in Appendix C.

Baselines. We select six baselines for comparison. The logits-based methods include popular **Perplexity** (Ren et al. 2023), commonly applied OOD detection score **Energy** (Liu et al. 2020), and **P(True)** (Lin, Hilton, and Evans 2022). The sampling-based methods contain Length-normalized Predictive Entropy (**LNPE**) (Malinin and Gales 2021), broadly acknowledged **Semantic Entropy** (Farquhar et al. 2024) and **EigenScore** (Chen et al. 2024). Besides, we compare the internal uncertainty method AttnScore from LLM-Check (Sriraman et al. 2024). These baselines’ implementation is detailed in Appendix C. We also compare the parameterized probe-based methods SAPLMA (Azaria and Mitchell 2023), Probe-LR (CH-Wang et al. 2024), and Probe-MM (Marks and Tegmark 2023) in Appendix E, F, and G.

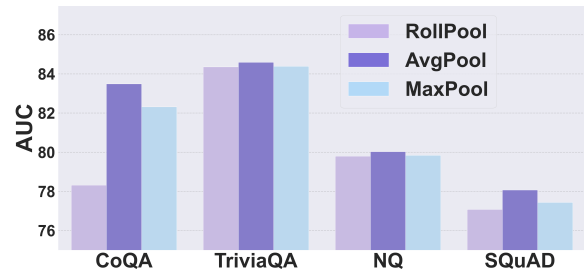


Figure 4: Comparison of base attribution strategies.

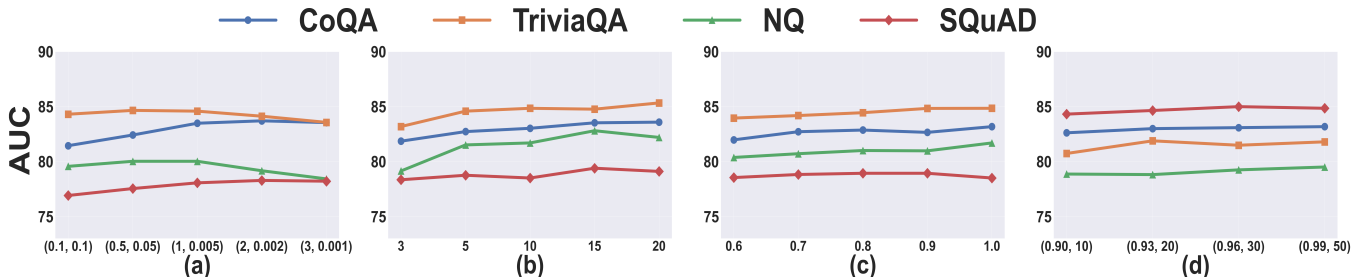


Figure 5: Performance under different hyperparameters. They are (a) our rescaling hypermeter group (α, ϵ), (b) number of Generation N, (c) temperature T , (d) sampling hyperparameter group (Top-P, Top-K).

Main Results

We select **AvgPool**, $\alpha = 1.0$, and $\epsilon = 0.005$ for our method. Table 1 reports the main results about the performance comparison of our **RePPL** and other baseline methods. From these results, we find that: (1) Our method achieves strong performance on hallucination detection. We reach the average AUC of **0.813** and **74.65%** accuracy at maximum G-Mean value on all individual datasets and all models. In addition, we also achieve an average AUC of **0.833** across 4 datasets (on the merge of 4 datasets). (2) Our method outperforms baselines, especially the strong baseline LNPE and EigenScore. Out of **60** evaluated metrics across datasets and models, our method ranks first in **46**, demonstrating its overall superiority. Compared to EigenScore, which ranks second and performs an average AUC of 0.795 & 72.78% average accuracy, Our method takes the leading position of detection performance by 2% improvement. And we also outperform in the merge of all datasets. (3) Our method exhibits high generalization across different datasets. Our method basically guarantees the AUC higher than 0.75, and the accuracy higher than 70%. (4) Our method also demonstrates good adaptability among different models, and it can scale to larger models like **Qwen2.5-14B-Instruct**. Therefore, **RePPL** owns strong hallucination detection performance. And it firmly supports the foundation of its explainability.

Ablation Studies

Computation Variation. To further verify the effectiveness of our proposed method, we conduct ablation experiments on Qwen2.5-7B-Instruct and illustrate them in this section. Firstly, we compare **InnerPPL** & **OuterPPL** and the vanilla perplexity version of our method (multiplying original Perplexity in Equation (7)) to prove the efficacy of our design. As Table 2 demonstrated, **RePPL** certainly improves performance over all its computational variations. Besides, **InnerPPL** and **RePPL** (Perplexity) derived from the original perplexity perform well individually.

Attribution Strategies. We also investigate the influence of different attribution methods in Figure Figure 4. An unexpected finding is that **AvgPool** performs best across all comparisons. Meanwhile, considering the lower computational complexity of **AvgPool**, we recommend it as the approach to derive the attribution map in our method.

Table 2: Ablation studies on Qwen2.5-7B-Instruct.

Ablations	Datasets			
	CoQA	TriviaQA	NQ	SQuAD
InnerPPL	83.5	80.1	76.3	75.3
OuterPPL	78.2	84.1	77.7	76.1
RePPL (Perplexity)	82.1	84.5	79.6	77.7
RePPL	83.8	84.6	80.0	78.1

Hyperparameters (α, ϵ). As for the hypermeter group (α, ϵ), the ablation results are shown in Figure 5(a). It indicates that our method remains robust under different hyperparameter settings. Given that (1.0, 0.005) achieves the best overall performance across 4 datasets, we recommend it as the default setting of our method.

Sensitivity to Sampling Hyperparameters

In this section, we extend our analysis to sensitivity to randomness in sampling, which is controlled by the following decoding hyperparameters. For efficiency considerations, a random one-fifth subset was taken from each dataset. The observed performance differs by no more than 1.5% from the main results. As Figure 5 (b) (c) (d) shows, randomness at different sampling hyperparameters affects our performance. However, this effect is limited as these curves display a moderately gradual ascent from lower randomness hyperparameters to higher ones. It indicates that our method is robust.

Explainability Analysis

Faithfulness Test

In line with previous XAI works (Hao et al. 2021; Chefer, Gur, and Wolf 2021; Ahtibat et al. 2024), we assess explanation faithfulness via perturbation tests that progressively mask low-scoring tokens. Here, we emphasize that explanation faithfulness is consistency with the model’s nature, not human cognition. The difference is that the assessment here focuses on which explanation more effectively highlights tokens that are more prone to inducing model hallucinations (uncertainty), rather than those that contribute more to the output (importance), hence, it needs detection performance as the indicator. A smaller detection performance drop across

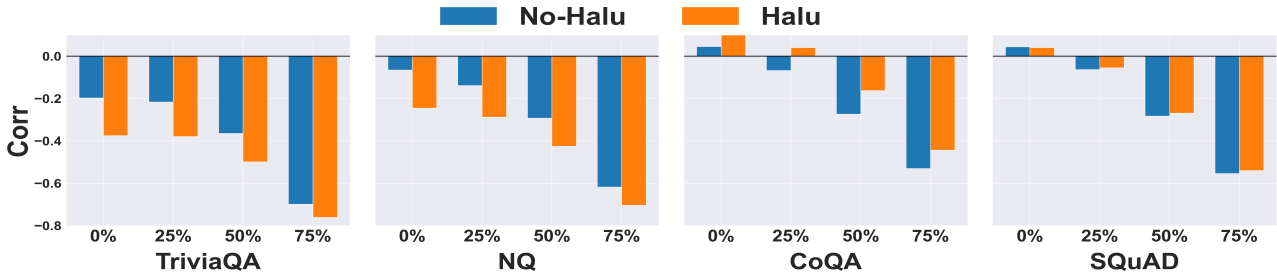


Figure 6: Average Spearman Correlation (Corr) between importance and uncertainty. X-axis correspond to different masking ratios. As can be seen, the negative average correlation is large at 75% masking ratios. On the QA datasets with context, this negative correlation is smaller in hallucinated ones while larger on the datasets without context.

Table 3: Faithfulness test on TriviaQA and SQuAD, AUC metric. 0%~75% correspond to different masking ratios.

Exp. Scores	TriviaQA				SQuAD			
	0%	25%	50%	75%	0%	25%	50%	75%
Raw Logits	66.9	67.1	65.5	63.7	51.2	51.0	50.8	50.2
AvgPool	60.0	60.0	59.3	57.6	51.3	51.5	52.0	53.0
MaxPool	62.6	62.7	62.3	62.4	50.2	50.8	52.1	54.5
RollPool	55.4	55.3	55.2	55.0	48.0	48.2	48.9	50.5
InnerPPL	79.7	79.4	79.1	78.6	74.2	73.9	73.8	73.2

masking ratios indicates greater faithfulness, and the absolute performance itself also reflects explanation reliability. To assess the faithfulness of identifying uncertainty-inducing tokens, we conduct the test in the input space (corresponding to log rescaled uncertainty score that consists **InnerPPL**), using one-fifth random subsets from TriviaQA and SQuAD. As for comparison, we take the raw logits in throughput of the input tokens, importance-oriented attribution scores of the three pooling strategies we adopt as explanation scores baselines. We steply mask these hallucination scores at ratios of 0%, 25%, 50%, and 75% and use the AUC metric for evaluation. Table 3 depicts a slight decrease in our method’s performance at different masking ratios, which proves the primary capability of rightfully attributing significant uncertainty-inducing tokens. On the contrary, all baselines show erratic drops, which show their inability to explain. Our method is even robust at the 75% masking ratio. This suggests its capacity to truly concern uncertainty-inducing tokens of hallucination.

Visual Explanation for Hallucination

We concatenate uncertainty scores that consist **InnerPPL** and **OuterPPL** as a token-wise and visualizable hallucination explanation. We take the log-rescaled uncertainty degree for visualization in Figure 7, which demonstrates good distinctness. More visual explanations are displayed in Appendix I.

Importance and Uncertainty

Coincidentally, during the computation process of our method, we first gain attribution-based importance and then derive the uncertainty about hallucination. We computed the average Spearman Correlation between importance scores

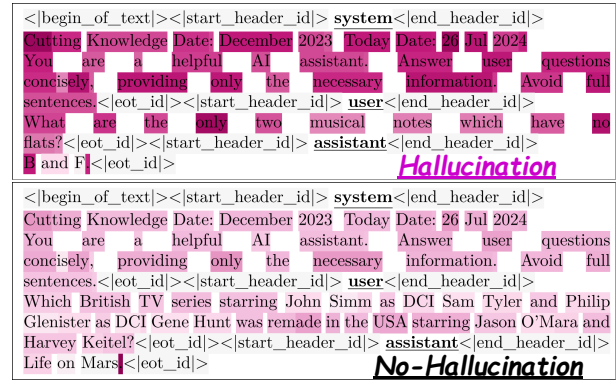


Figure 7: Visual explanations of the whole QA process on TriviaQA. The upper one is detected as a hallucination by **RePPL**. The lower one is non-hallucinated. Here, we mask the special token for better presentation.

and uncertainty scores on the same data of ablation studies (detailed in Appendix J). Results in Figure 6 demonstrate two noteworthy findings: (1) **Uncertainty is negatively correlated to importance**. The negative correlation indicates uncertainty that induces hallucination, bringing chaos to the correct attention pattern. (2) **This correlation corresponds to different hallucination types**. The different average correlation on the dataset with/without context illustrates a discrepant hallucination pattern about factual (external) and contextual (internal) ones. Overall, these findings describe the disorder in the chaotic attention pattern when LLM tends to hallucinate. And demonstrate the potential usage of our explanation scores as a viable tool.

Conclusion

In conclusion, we are motivated by the explainability limitations of the current hallucination detection method, and introduce a fresh perspective to exploit uncertainty in semantic propagation and language generation. Based on that, we propose our **RePPL** to utilize the discrepancy between the attribution of different sampled generations and combine refined generation confidence. These designs equip our method with our hierarchical distinctness for better detection and token-level uncertainty correspondence for explanation.

The experiments indicate that our method achieves strong detection performance, and it is able to highlight uncertainty-inducing tokens as an explanation. We hope our insights, even drawbacks, can better motivate future research in this domain to better tackle the hallucination of LLM and build more trustworthy AI systems in future.

References

- Abnar, S.; and Zuidema, W. H. 2020. Quantifying Attention Flow in Transformers. In Jurafsky, D.; Chai, J.; Schluter, N.; and Tetreault, J. R., eds., *Proceedings of the 58th Annual Meeting of the Association for Computational Linguistics, ACL 2020, Online, July 5-10, 2020*, 4190–4197. Association for Computational Linguistics.
- Achtibat, R.; Hatefi, S. M. V.; Dreyer, M.; Jain, A.; Wiegand, T.; Lopuschkin, S.; and Samek, W. 2024. AttnLRP: Attention-Aware Layer-Wise Relevance Propagation for Transformers. In *Forty-first International Conference on Machine Learning, ICML 2024, Vienna, Austria, July 21-27, 2024*. OpenReview.net.
- Azaria, A.; and Mitchell, T. M. 2023. The Internal State of an LLM Knows When It’s Lying. In Bouamor, H.; Pino, J.; and Bali, K., eds., *Findings of the Association for Computational Linguistics: EMNLP 2023, Singapore, December 6-10, 2023*, 967–976. Association for Computational Linguistics.
- CH-Wang, S.; Durme, B. V.; Eisner, J.; and Kedzie, C. 2024. Do Androids Know They’re Only Dreaming of Electric Sheep? In Ku, L.; Martins, A.; and Srikumar, V., eds., *Findings of the Association for Computational Linguistics, ACL 2024, Bangkok, Thailand and virtual meeting, August 11-16, 2024*, 4401–4420. Association for Computational Linguistics.
- Chefer, H.; Gur, S.; and Wolf, L. 2021. Generic Attention-model Explainability for Interpreting Bi-Modal and Encoder-Decoder Transformers. In *2021 IEEE/CVF International Conference on Computer Vision, ICCV 2021, Montreal, QC, Canada, October 10-17, 2021*, 387–396. IEEE.
- Chen, C.; Liu, K.; Chen, Z.; Gu, Y.; Wu, Y.; Tao, M.; Fu, Z.; and Ye, J. 2024. INSIDE: LLMs’ Internal States Retain the Power of Hallucination Detection. In *The Twelfth International Conference on Learning Representations, ICLR 2024, Vienna, Austria, May 7-11, 2024*. OpenReview.net.
- Du, X.; Xiao, C.; and Li, S. 2024. HaloScope: Harnessing Unlabeled LLM Generations for Hallucination Detection. In Globersons, A.; Mackey, L.; Belgrave, D.; Fan, A.; Paquet, U.; Tomczak, J. M.; and Zhang, C., eds., *Advances in Neural Information Processing Systems 38: Annual Conference on Neural Information Processing Systems 2024, NeurIPS 2024, Vancouver, BC, Canada, December 10 - 15, 2024*.
- Fakour, F.; Mosleh, A.; and Ramezani, R. 2024. A Structured Review of Literature on Uncertainty in Machine Learning & Deep Learning. *CoRR*, abs/2406.00332.
- Farquhar, S.; Kossen, J.; Kuhn, L.; and Gal, Y. 2024. Detecting hallucinations in large language models using semantic entropy. *Nat.*, 630(8017): 625–630.
- Ferrando, J.; Obeso, O. B.; Rajamanoharan, S.; and Nanda, N. 2025. Do I Know This Entity? Knowledge Awareness and Hallucinations in Language Models. In *The Thirteenth International Conference on Learning Representations, ICLR 2025, Singapore, April 24-28, 2025*. OpenReview.net.
- Grattafiori, A.; Dubey, A.; Jauhri, A.; Pandey, A.; Kadian, A.; Al-Dahle, A.; Letman, A.; Mathur, A.; Schelten, A.; Vaughan, A.; et al. 2024. The llama 3 herd of models. *arXiv preprint arXiv:2407.21783*.
- Hao, Y.; Dong, L.; Wei, F.; and Xu, K. 2021. Self-Attention Attribution: Interpreting Information Interactions Inside Transformer. In *Thirty-Fifth AAAI Conference on Artificial Intelligence, AAAI 2021, Thirty-Third Conference on Innovative Applications of Artificial Intelligence, IAAI 2021, The Eleventh Symposium on Educational Advances in Artificial Intelligence, EAAI 2021, Virtual Event, February 2-9, 2021*, 12963–12971. AAAI Press.
- He, H.; and Garcia, E. A. 2009. Learning from Imbalanced Data. *IEEE Transactions on Knowledge and Data Engineering*, 21(9): 1263–1284.
- Joshi, M.; Choi, E.; Weld, D.; and Zettlemoyer, L. 2017. TriviaQA: A Large Scale Distantly Supervised Challenge Dataset for Reading Comprehension. In Barzilay, R.; and Kan, M.-Y., eds., *Proceedings of the 55th Annual Meeting of the Association for Computational Linguistics (Volume 1: Long Papers)*, 1601–1611. Vancouver, Canada: Association for Computational Linguistics.
- Kwiatkowski, T.; Palomaki, J.; Redfield, O.; Collins, M.; Parikh, A.; Alberti, C.; Epstein, D.; Polosukhin, I.; Devlin, J.; Lee, K.; Toutanova, K.; Jones, L.; Kelcey, M.; Chang, M.-W.; Dai, A. M.; Uszkoreit, J.; Le, Q.; and Petrov, S. 2019. Natural Questions: A Benchmark for Question Answering Research. *Transactions of the Association for Computational Linguistics*, 7: 452–466.
- Li, H.; Dong, Q.; Chen, J.; Su, H.; Zhou, Y.; Ai, Q.; Ye, Z.; and Liu, Y. 2024. LLMs-as-Judges: A Comprehensive Survey on LLM-based Evaluation Methods. *CoRR*, abs/2412.05579.
- Lin, C.-Y. 2004. ROUGE: A Package for Automatic Evaluation of Summaries. In *Text Summarization Branches Out*, 74–81. Barcelona, Spain: Association for Computational Linguistics.
- Lin, S.; Hilton, J.; and Evans, O. 2022. Teaching Models to Express Their Uncertainty in Words. *Trans. Mach. Learn. Res.*, 2022.
- Liu, J.; Chen, S.; Cheng, Y.; and He, J. 2024a. On the universal truthfulness hyperplane inside llms. *arXiv preprint arXiv:2407.08582*.
- Liu, W.; Wang, X.; Owens, J. D.; and Li, Y. 2020. Energy-based Out-of-distribution Detection. In Larochelle, H.; Ranzato, M.; Hadsell, R.; Balcan, M.; and Lin, H., eds., *Advances in Neural Information Processing Systems 33: Annual Conference on Neural Information Processing Systems 2020, NeurIPS 2020, December 6-12, 2020, virtual*.
- Liu, X.; Xu, N.; Chen, M.; and Xiao, C. 2024b. AutoDAN: Generating Stealthy Jailbreak Prompts on Aligned Large Language Models. In *The Twelfth International Conference on Learning Representations, ICLR 2024, Vienna, Austria, May 7-11, 2024*. OpenReview.net.

- Lundberg, S. M.; Erion, G. G.; and Lee, S. 2018. Consistent Individualized Feature Attribution for Tree Ensembles. *CoRR*, abs/1802.03888.
- Lundberg, S. M.; and Lee, S. 2017. A Unified Approach to Interpreting Model Predictions. In Guyon, I.; von Luxburg, U.; Bengio, S.; Wallach, H. M.; Fergus, R.; Vishwanathan, S. V. N.; and Garnett, R., eds., *Advances in Neural Information Processing Systems 30: Annual Conference on Neural Information Processing Systems 2017, December 4-9, 2017, Long Beach, CA, USA*, 4765–4774.
- Ma, H.; Chen, J.; Wang, G.; and Zhang, C. 2025. Estimating LLM Uncertainty with Logits. *CoRR*, abs/2502.00290.
- Malinin, A.; and Gales, M. J. F. 2021. Uncertainty Estimation in Autoregressive Structured Prediction. In *9th International Conference on Learning Representations, ICLR 2021, Virtual Event, Austria, May 3-7, 2021*. OpenReview.net.
- Marks, S.; and Tegmark, M. 2023. The Geometry of Truth: Emergent Linear Structure in Large Language Model Representations of True/False Datasets. *CoRR*, abs/2310.06824.
- OpenAI. 2023. ChatGPT. Version GPT-4, Large language model.
- Orgad, H.; Toker, M.; Gekhman, Z.; Reichart, R.; Szpektor, I.; Kotek, H.; and Belinkov, Y. 2024. LLMs know more than they show: On the intrinsic representation of LLM hallucinations. *arXiv preprint arXiv:2410.02707*.
- Rajpurkar, P.; Zhang, J.; Lopyrev, K.; and Liang, P. 2016. SQuAD: 100,000+ Questions for Machine Comprehension of Text. In Su, J.; Duh, K.; and Carreras, X., eds., *Proceedings of the 2016 Conference on Empirical Methods in Natural Language Processing*, 2383–2392. Austin, Texas: Association for Computational Linguistics.
- Reddy, S.; Chen, D.; and Manning, C. D. 2019. CoQA: A Conversational Question Answering Challenge. *Trans. Assoc. Comput. Linguistics*, 7: 249–266.
- Reimers, N.; and Gurevych, I. 2019. Sentence-BERT: Sentence Embeddings using Siamese BERT-Networks. In *Proceedings of the 2019 Conference on Empirical Methods in Natural Language Processing*, 3982–3992.
- Ren, J.; Luo, J.; Zhao, Y.; Krishna, K.; Saleh, M.; Lakshminarayanan, B.; and Liu, P. J. 2023. Out-of-Distribution Detection and Selective Generation for Conditional Language Models. In *The Eleventh International Conference on Learning Representations, ICLR 2023, Kigali, Rwanda, May 1-5, 2023*. OpenReview.net.
- Ribeiro, M. T.; Singh, S.; and Guestrin, C. 2016. "Why Should I Trust You?": Explaining the Predictions of Any Classifier. In Krishnapuram, B.; Shah, M.; Smola, A. J.; Aggarwal, C. C.; Shen, D.; and Rastogi, R., eds., *Proceedings of the 22nd ACM SIGKDD International Conference on Knowledge Discovery and Data Mining, San Francisco, CA, USA, August 13-17, 2016*, 1135–1144. ACM.
- Spearman, C. 1904. The Proof and Measurement of Association between Two Things. *The American Journal of Psychology*, 15(1): 72–101.
- Sriramanan, G.; Bharti, S.; Sadasivan, V. S.; Saha, S.; Katakinda, P.; and Feizi, S. 2024. LLM-Check: Investigating Detection of Hallucinations in Large Language Models. In Globerson, A.; Mackey, L.; Belgrave, D.; Fan, A.; Paquet, U.; Tomczak, J.; and Zhang, C., eds., *Advances in Neural Information Processing Systems*, volume 37, 34188–34216. Curran Associates, Inc.
- Sun, S.; Chen, C.; and Carin, L. 2017. Learning Structured Weight Uncertainty in Bayesian Neural Networks. In Singh, A.; and Zhu, J., eds., *Proceedings of the 20th International Conference on Artificial Intelligence and Statistics*, volume 54 of *Proceedings of Machine Learning Research*, 1283–1292. PMLR.
- Vashurin, R.; Fadeeva, E.; Vazhentsev, A.; Rvanova, L.; Vasilev, D.; Tsvigun, A.; Petrakov, S.; Xing, R.; Sadallah, A. B.; Grishchenkov, K.; Panchenko, A.; Baldwin, T.; Nakov, P.; Panov, M.; and Shelmanov, A. 2025. Benchmarking Uncertainty Quantification Methods for Large Language Models with LM-Polygraph. *Trans. Assoc. Comput. Linguistics*, 13: 220–248.
- Wang, Y.; Li, H.; Zou, H.; Zhang, J.; He, X.; Li, Q.; and Xu, K. 2024. FacLens: Transferable Probe for Foreseeing Non-Factuality in Large Language Models. *arXiv:2406.05328*.
- Xu, X.; Kong, K.; Liu, N.; Cui, L.; Wang, D.; Zhang, J.; and Kankanhalli, M. S. 2024. An LLM can Fool Itself: A Prompt-Based Adversarial Attack. In *The Twelfth International Conference on Learning Representations, ICLR 2024, Vienna, Austria, May 7-11, 2024*. OpenReview.net.
- Yang, A.; Yang, B.; Zhang, B.; Hui, B.; Zheng, B.; Yu, B.; Li, C.; Liu, D.; Huang, F.; Wei, H.; et al. 2024. Qwen2. 5 technical report. *arXiv preprint arXiv:2412.15115*.
- Yu, L.; Cao, M.; Cheung, J. C. K.; and Dong, Y. 2024. Mechanistic Understanding and Mitigation of Language Model Non-Factual Hallucinations. In Al-Onaizan, Y.; Bansal, M.; and Chen, Y., eds., *Findings of the Association for Computational Linguistics: EMNLP 2024, Miami, Florida, USA, November 12-16, 2024*, 7943–7956. Association for Computational Linguistics.
- Zhang, H.; Diao, S.; Lin, Y.; Fung, Y.; Lian, Q.; Wang, X.; Chen, Y.; Ji, H.; and Zhang, T. 2024. R-tuning: Instructing large language models to say 'I don't know'. In *Proceedings of the 2024 Conference of the North American Chapter of the Association for Computational Linguistics: Human Language Technologies (Volume 1: Long Papers)*, 7106–7132.
- Zhang, Y.; Li, S.; Qian, C.; Liu, J.; Yu, P.; Han, C.; Fung, Y. R.; McKeown, K.; Zhai, C.; Li, M.; and Ji, H. 2025. The Law of Knowledge Overshadowing: Towards Understanding, Predicting, and Preventing LLM Hallucination. *arXiv:2502.16143*.

A Implementation Details

We conduct all of our experiments on an NVIDIA H100 GPU, with full precision FP32. All of the implementations are based on transformers library of Huggingface. And all generations include related internal states and attention maps are derived from the `.generate(...)` of `GenerateMixin` Class (Which is the part of the `Model` Class). In addition, attention maps can be returned with the `attn_implementation="eager"` when loading the

Table 4: Evaluation results of different methods on various datasets using AUC, accuracy at threshold of max G-Mean (Acc), and Spearman Correlation (Corr) metrics. ROUGE-L (f1-measure) is the correctness measure. All values are percentages. The best performances of non-parameterized methods are in bold, and the best performances of parameterized methods (*) are underlined.

Models	Datasets	CoQA				TriviaQA				NQ				SQuAD				ALL			
		AUC	Acc	Corr	PRR																
LLaMA-3.1-8B-Instruct	Perplexity	70.4	65.0	34.6	44.6	78.5	71.3	53.7	62.9	74.8	69.1	42.9	49.3	71.2	65.8	33.8	30.6	76.2	69.5	47.1	53.3
	Energy	68.1	62.1	30.9	41.7	68.0	63.6	35.6	40.5	65.3	62.7	28.8	32.2	70.7	66.2	35.4	47.2	71.9	66.0	39.7	48.8
	P(True)	66.4	61.6	29.6	39.3	77.9	71.1	50.7	60.0	69.3	65.8	35.6	38.9	68.6	61.0	27.5	38.5	74.4	68.1	44.0	52.6
	LNPE	75.4	68.1	43.6	51.9	81.0	73.4	56.9	66.5	76.1	69.5	43.1	50.0	73.5	70.7	37.7	35.5	79.3	72.4	52.1	57.4
	Semantic Entropy	75.3	70.0	44.2	52.2	75.2	69.2	44.3	53.4	66.1	64.1	25.7	31.4	71.6	73.2	33.3	35.8	76.1	70.7	45.5	52.7
	EigenScore	79.0	73.8	49.0	58.6	80.8	73.7	55.2	65.1	71.9	70.4	33.6	42.4	80.4	73.4	51.9	62.7	79.2	71.2	51.1	60.6
	AttnScore	71.9	68.5	38.7	37.9	72.9	67.0	40.9	44.5	62.5	59.8	16.4	24.8	67.2	64.5	28.8	28.8	59.7	54.6	17.1	25.3
	RePPL (Ours)	83.5	77.0	60.6	67.0	85.2	76.9	62.5	71.1	75.3	69.4	37.9	48.6	76.0	70.8	48.1	40.6	82.8	75.5	58.9	63.6
	SAPLMA*	<u>88.5</u>	<u>80.7</u>	<u>69.2</u>	<u>78.4</u>	<u>90.2</u>	<u>82.5</u>	<u>68.1</u>	<u>78.4</u>	<u>72.9</u>	<u>67.2</u>	<u>34.9</u>	<u>45.1</u>	<u>87.2</u>	<u>79.3</u>	<u>59.0</u>	<u>72.6</u>	88.2	80.5	66.0	75.2
	Probe-LR*	88.1	80.1	69.2	<u>79.0</u>	90.0	82.3	<u>68.7</u>	78.3	<u>76.5</u>	<u>69.4</u>	<u>41.1</u>	<u>51.8</u>	86.8	79.0	58.3	69.6	<u>88.6</u>	<u>80.6</u>	<u>67.8</u>	<u>76.7</u>
	Probe-MM*	79.6	72.4	55.4	61.9	83.4	75.3	60.6	71.1	70.1	63.9	29.6	37.4	81.6	76.4	50.2	62.3	73.9	67.9	42.8	46.4
Qwen-2.5-7B-Instruct	Perplexity	74.4	67.6	44.9	56.2	83.5	75.6	60.4	70.4	75.5	69.6	38.8	41.7	74.1	69.1	46.9	49.6	81.2	73.0	58.1	65.6
	Energy	60.2	57.3	16.1	21.7	77.6	70.8	49.4	52.5	64.6	57.5	27.6	22.3	60.8	58.7	15.9	19.4	71.0	65.8	39.8	42.1
	P(True)	57.7	57.2	16.4	15.8	80.8	75.0	57.3	65.4	65.1	63.9	26.5	32.3	59.2	60.3	14.2	20.4	74.1	69.8	46.4	49.6
	LNPE	76.3	69.9	48.0	58.5	83.7	76.0	60.6	70.8	76.4	66.6	40.1	44.3	75.1	70.2	48.1	50.5	82.1	74.3	59.5	66.1
	Semantic Entropy	74.2	73.8	40.9	40.2	77.7	76.0	49.4	54.7	71.8	73.1	30.3	36.4	65.9	79.3	22.2	24.3	77.7	76.4	49.0	50.9
	EigenScore	81.7	76.0	56.4	58.4	82.6	75.9	57.7	60.8	77.4	72.1	37.4	41.0	78.3	74.6	50.6	53.3	82.8	76.5	58.3	62.2
	AttnScore	71.0	65.9	34.6	39.6	60.9	58.0	18.7	18.8	62.2	56.2	13.8	14.1	71.1	65.3	35.8	42.2	60.8	59.4	21.8	31.0
	RePPL (Ours)	81.2	73.7	57.1	64.0	84.1	76.0	61.1	70.2	77.7	67.0	37.8	43.8	77.1	70.5	51.6	52.6	83.3	75.4	60.8	67.7
	SAPLMA*	<u>91.2</u>	<u>83.0</u>	<u>74.3</u>	<u>82.6</u>	<u>90.6</u>	<u>83.1</u>	<u>71.7</u>	<u>81.8</u>	<u>83.4</u>	<u>73.6</u>	<u>45.3</u>	<u>57.6</u>	<u>88.0</u>	<u>78.3</u>	<u>65.8</u>	<u>74.6</u>	<u>90.4</u>	<u>83.0</u>	<u>70.6</u>	<u>79.2</u>
	Probe-LR*	88.3	80.4	70.0	76.6	86.8	78.8	65.3	74.7	79.7	72.6	40.1	49.2	83.4	76.0	59.1	66.2	87.8	79.9	67.2	75.6
	Probe-MM*	73.9	68.9	43.8	48.9	76.6	71.5	50.2	50.4	74.8	71.0	35.0	34.3	76.3	71.5	49.2	49.8	73.4	67.8	41.2	39.8
Qwen-2.5-14B-Instruct	Perplexity	72.8	66.9	44.9	48.2	80.8	73.2	57.0	66.0	74.3	68.0	38.7	44.1	75.0	67.7	49.2	51.8	77.0	70.3	52.6	57.8
	Energy	61.1	57.0	27.4	19.1	63.5	61.0	28.4	26.4	60.0	56.7	22.8	21.9	60.0	58.8	20.8	21.4	57.4	54.1	22.8	19.4
	P(True)	60.8	57.9	27.0	21.4	72.4	71.0	44.8	40.9	62.0	65.2	28.3	25.6	54.0	55.9	9.4	2.4	63.1	62.6	33.8	23.4
	LNPE	74.2	68.0	47.4	49.2	81.9	74.6	58.7	66.1	75.2	68.9	39.7	43.2	76.4	69.8	51.4	53.5	78.1	71.2	54.6	58.8
	Semantic Entropy	67.8	62.5	36.1	23.7	76.7	76.3	47.0	47.0	69.9	72.2	30.3	33.5	66.4	72.3	29.0	24.7	71.8	70.9	41.8	36.5
	EigenScore	80.1	72.2	56.0	51.1	82.6	77.2	57.1	60.7	76.4	72.2	37.0	37.3	81.5	74.4	58.5	57.4	81.4	74.9	56.0	56.3
	AttnScore	53.2	51.6	9.8	6.4	63.2	60.1	24.6	26.5	63.0	59.8	20.5	19.0	55.1	53.5	9.0	3.6	60.7	59.3	12.9	23.9
	RePPL (Ours)	76.3	71.2	50.6	52.7	84.1	76.2	61.1	68.6	77.5	69.2	39.1	44.3	80.6	72.6	58.9	58.0	80.7	73.4	56.9	61.2
	SAPLMA*	<u>90.8</u>	<u>82.7</u>	<u>71.9</u>	<u>82.5</u>	<u>92.6</u>	<u>85.1</u>	<u>73.7</u>	<u>83.2</u>	<u>81.9</u>	<u>73.0</u>	<u>43.5</u>	<u>55.7</u>	<u>91.9</u>	<u>86.3</u>	<u>77.4</u>	<u>83.1</u>	<u>91.4</u>	<u>83.8</u>	<u>72.8</u>	<u>81.7</u>
	Probe-LR*	89.4	82.4	69.1	80.1	90.2	82.7	69.8	78.9	78.9	72.4	38.9	48.3	91.1	85.3	73.7	78.2	89.7	82.1	68.1	77.7
	Probe-MM*	74.1	72.9	43.4	45.0	55.9	61.8	22.3	13.0	54.7	35.5	12.8	3.5	68.3	77.4	47.6	26.1	64.1	62.8	23.8	12.7

model’s weights. For model weights of Llama-3.1-8B-Instruct, Qwen2.5-7B-Instruct, Qwen2.5-14B-Instruct, and the sentence embedding model all-MiniLM-L6-v2, we choose the open-source weights from their Huggingface repositories. For the ROUGE metric, we select the standard implementation of Google Research. All metrics we use are adopted or consist of the implementation of scikit-learn library.

B Inference Settings

Since we select the instruction-finetuned model for experiments, to more closely simulate practical scenarios, we adopt the chat template for generation. In the system prompt, we constrain the model to only answer key information by the instructions. As a result, the model’s responses are closer to

the standard answer of QA pairs. The input format of QA pairs is shown as follows:

System Prompt: *You are a helpful AI assistant. Answer user questions concisely, providing only the necessary information. Avoid full sentences.*

User Prompt: <Question>

The input format with context is:

System Prompt: *You are a helpful AI assistant. Answer user questions based on provided context concisely, providing only the necessary information. Avoid full sentences.*

User Prompt: *Context:* <Context> *Question:* <Question>

Table 5: Extra evaluation results of comparison between different parameterized methods (*) and ours on various datasets, using AUC, accuracy at threshold of max G-Mean (Acc), and Spearman Correlation (Corr) metrics. Embedding similarity is the correctness measure. All values are in percentages.

Models	Datasets Methods	CoQA				TriviaQA				NQ				SQuAD				ALL			
		AUC	Acc	Corr	PRR	AUC	Acc	Corr	PRR	AUC	Acc	Corr	PRR	AUC	Acc	Corr	PRR	AUC	Acc	Corr	PRR
LLaMA-3.1-8B-Instruct	RePPL (Ours)	85.2	77.4	61.8	70.7	86.0	78.6	63.2	73.9	79.3	69.9	47.4	51.9	76.0	71.7	45.1	40.6	83.6	76.3	60.0	66.4
	SAPLMA*	88.5	81.1	66.7	80.1	87.7	79.3	67.6	79.4	74.3	69.6	40.4	45.6	79.8	73.2	52.5	70.7	85.6	78.4	64.4	75.4
	Probe-LR*	89.4	82.2	67.9	81.7	88.5	80.5	68.9	80.7	79.1	70.3	45.9	52.1	79.0	72.4	51.7	65.6	87.1	79.9	66.7	77.7
	Probe-MM*	85.0	77.7	62.1	73.8	86.5	78.1	63.4	75.4	77.1	67.6	31.2	36.2	75.3	68.3	46.2	61.8	77.5	70.4	48.8	53.4
Qwen-2.5-7B-Instruct	RePPL (Ours)	83.5	77.0	58.4	67.2	84.6	76.3	62.4	73.3	80.0	73.6	45.8	46.5	78.1	71.9	47.8	54.9	83.7	75.9	60.9	68.9
	SAPLMA*	92.0	84.7	73.1	82.3	89.8	82.5	71.7	81.9	84.7	75.5	50.5	56.8	84.1	78.2	60.0	72.6	89.4	82.5	70.8	78.3
	Probe-LR*	90.9	83.5	70.2	77.6	86.0	78.0	64.8	74.9	81.3	73.5	42.9	48.9	80.5	75.1	53.6	63.7	87.7	80.0	66.9	75.2
	Probe-MM*	80.5	73.6	52.3	57.5	77.2	72.6	53.5	55.6	76.9	69.9	30.3	30.8	73.9	71.0	46.2	52.9	75.9	70.6	47.4	45.9
Qwen-2.5-14B-Instruct	RePPL (Ours)	79.7	76.6	43.0	47.9	84.8	76.8	62.2	71.9	80.0	71.7	51.4	50.1	81.3	74.4	54.7	56.8	82.5	75.7	56.0	60.4
	SAPLMA*	96.5	92.0	68.5	79.0	90.7	82.9	73.4	83.4	83.7	77.1	54.9	58.3	90.2	83.4	72.3	78.8	91.5	84.3	73.1	80.8
	Probe-LR*	95.4	88.6	66.9	77.2	88.8	80.9	70.2	80.3	80.5	71.9	49.4	50.8	87.8	80.9	68.6	74.2	90.6	82.4	71.4	78.4
	Probe-MM*	85.0	78.9	43.9	42.0	55.2	50.5	26.7	17.2	54.6	25.5	24.3	6.8	64.5	62.0	40.9	22.1	66.3	56.2	38.0	20.7

C Details of Metrics

AUC. Area Under the Receiver Operating Characteristic Curve (AUC) is the classic metric for measuring the performance of a classifier, specifically the score-based classifier without a preset threshold.

Acc. Our accuracy (Acc) is the accuracy at the threshold spot that receives maximum **G-Mean** (He and Garcia 2009) value. This is computed as $\text{G-Mean} = \sqrt{\text{TPR} \times (1 - \text{FPR})}$, where TPR is true positive rate and FPR is false positive rate. When **G-Mean** reaches the maximum, the performance of the score-based classifier achieves its best at the corresponding threshold, especially in the imbalanced scenarios (He and Garcia 2009). In other words, the accuracy for predicting the positive class and the negative class has achieved the geometric mean optimal value. Hence, the accuracy at this specified threshold reflects the overall performance.

Corr. We select Spearman Correlation (Spearman 1904) (Corr) as our performance metric. It non-linearly embodies the overall similarity between the hallucination detection score and the correctness measure score (soft version of hallucination ground truth) on the whole dataset.

PRR. The Prediction Rejection Ratio (Vashurin et al. 2025) (PRR) is a metric designed to evaluate the effectiveness of an uncertainty quantification method by assessing how well uncertain predictions correspond to different quality responses of LLM (quality here is the score of the two correctness measures we adopt). It firstly computes from a prediction-rejection curve, which plots the average quality score of the correctness measure when the most uncertain predictions (the biggest uncertain scores for hallucination detection) are progressively discarded. Let Area_{unc} denote the area under this rejection curve induced by the uncertainty scores. In contrast, we also plot the curve that first discards the lowest quality score as an optimal rejection strategy curve for comparison.

Let $\text{Area}_{\text{oracle}}$ denote the area under the optimal rejection strategy that discards the lowest-quality samples first. PRR is defined as (Area_{rnd} is the area for a randomly permuted uncertainty score):

$$\text{PRR} = \frac{\text{Area}_{\text{unc}} - \text{Area}_{\text{rnd}}}{\text{Area}_{\text{oracle}} - \text{Area}_{\text{rnd}}}.$$

D Baseline Implementation

Perplexity. We compute perplexity (Ren et al. 2023) as the following equation:

$$\text{PPL} = -\frac{1}{S} \sum_i^S \log(p),$$

here, S is the length of generation and p is logits of generation tokens.

Energy. Energy score (Liu et al. 2020) is the result of exp-log rescaling:

$$\text{Energy} = \frac{1}{S} \sum_{i=1}^S \log\left(\sum_j \exp(p)\right),$$

which protrude the most uncertain logits.

P(True). It gives LLM a prompt to let LLM answer the question about whether the candidate answers hallucinate (Lin, Hilton, and Evans 2022). We prompt LLM as follows:

System Prompt: *You are a helpful assistant. You are asked to determine whether the possible answer correctly responds to the entire question, which may include context.*

User Prompt: *Entire Question (may include context):*
<Question>

Possible answer: <Candidate Response>

Does the possible answer correctly respond to the question above? Answer ‘Yes’ or ‘No’ only:

Then, if the "Yes" token (or equivalent tokens) appears in answers, we count the probability of this token $P(y = \text{"Yes"})$ as the hallucination score for detection.

Length-Normalized Predictive Entropy (LNPE). LNPE (Malinin and Gales 2021) proposes to measure sequence-level uncertainty by calculating the expectation of uncertainty in multiple generations, which is mathematically equivalent to the average of the PPL across different generations. It is computed as:

$$\text{LNPE} = -\frac{1}{N} \sum_{m=1}^N \frac{1}{S_n} \sum_{t=1}^{S_n} \log(p).$$

Here, $1, 2, \dots, n$ is the index of each generation in N times and the S_n is the corresponding generation length.

Semantic Entropy. The core idea of this method is to cluster the uncertainty of similar outputs then accumulate overall uncertainty that avoids distortion in the direct average accumulation (Farquhar et al. 2024). It is:

$$H_m = -\sum_{i=1}^{C_m} p_i \log p_i,$$

$$\text{Semantic Entropy} = \frac{1}{M} \sum_{j=1}^m H_j.$$

Therein, we have M clusters $1, 2, \dots, m$, each has C_m numbers of outputs which contain H_m semantic entropy of the cluster.

EigenScore. This estimates the hallucination degree of generated outputs based on the semantic dispersion in the sentence embedding space (Chen et al. 2024). It computes the covariance matrix of N generated sentence embeddings and then uses the log and determinant of the regularized covariance matrix to capture the diversity and confidence of the generation. It is defined as:

$$\text{EigenScore} = \frac{1}{N} \log \det(\Sigma + \alpha \cdot \mathbf{I}_N),$$

where $\Sigma = \mathbf{Z}^\top \mathbf{J}_d \mathbf{Z} \in \mathbb{R}^{N \times N}$ is the centered covariance matrix of N sentence embeddings $\mathbf{Z} = [z_1, \dots, z_n] \in \mathbb{R}^{d \times N}$, $\mathbf{J}_d = \mathbf{I}_d - \frac{1}{N} \mathbf{I}_N \mathbf{I}_N^\top$, and $\alpha \cdot \mathbf{I}_N$ is a small regularization term added to make the covariance matrix full rank. z_n is the middle layer hidden state of the last token.

AttnScore. AttnScore is a method that leverages internal components of the self-attention mechanism to detect hallucinations, which is the best method in the LLM-Check toolbox (Sriramanan et al. 2024). Instead of using hidden states, it analyzes the lower-triangular kernel matrices from each self-attention head. For a given input-output sequence $x_p \oplus x$ of length m , let $\text{Ker}^i \in \mathbb{R}^{m \times m}$ denote the lower-triangular kernel matrix of the self-attention map from attention head $i \in \{1, \dots, a\}$. Each matrix is computed via a Softmax over

scaled dot products and has non-negative diagonal entries. Since these diagonals match the eigenvalues of Ker^i , we compute the log-determinant of each head as the sum of logarithms of its diagonal entries. The final AttnScore is obtained by averaging these log-determinants across all a heads and normalizing by the sequence length m :

$$\text{AttnScore} = \frac{1}{a \cdot m} \sum_{i=1}^a \sum_{j=1}^m \log \text{Ker}_{jj}^i.$$

SAPLMA. SAPLMA (Azaria and Mitchell 2023) is a method for hallucination prediction that leverages the last hidden state (corresponding to the last token) activations at middle-high layers from LLMs. Specifically, we train a feedforward neural network classifier with a 3-layer MLP architecture (dimensions decrease exponentially) for 10 epochs using the Adam optimizer and the Binary Cross Entropy Loss, with the AUC metric being the proof of saving the optimal checkpoint. All data is collected from the train set of the dataset we adopt (we illustrate in the main text that we use the validation set of this dataset for performance comparison), at a size of 4 times the validation set we use for comparison (all parameterized methods use this same training data).

Probe-LR. It uses a logistic regression (LR) probe (CH-Wang et al. 2024) at the last hidden state (corresponding to the last token) activations at middle layers from LLMs to detect hallucinations. Given a prompt and generated response, we extract the hidden states in the middle layer from the LLM during generation. We adopt the same training strategy of SAPLMA to train it (the optimal learning rate is different).

Probe-MM. To distinguish between hallucinated (H) and non-hallucinated (NH) instances in the training set, we first derive the average activations for each group separately. That is the core idea of the Mass-Mean-style (MM) probe (Marks and Tegmark 2023). Specifically, we take the last token in the middle layer, we compute the average response μ over all hallucinated training samples $\mathcal{D}_{\text{train}}^H$, and ν over all non-hallucinated samples $\mathcal{D}_{\text{train}}^{NH}$:

$$\mu = \frac{1}{|\mathcal{D}_{\text{train}}^H|} \sum_{t \in \mathcal{D}_{\text{train}}^H} x_t^H,$$

$$\nu = \frac{1}{|\mathcal{D}_{\text{train}}^{NH}|} \sum_{q \in \mathcal{D}_{\text{train}}^{NH}} x_q^{NH}.$$

Next, we define a contrastive signal by taking the difference between the mean activations of the H and NH classes:

$$\theta = \mu - \nu.$$

Finally, we can use θ as the weights of the linear probe $p_{\text{hallu}}(x) = \theta x$ to judge whether the x corresponding response is hallucinated or not.

E ROUGE-based Comparison

The results of ROUGE-L (f-measure) as the correctness measure are listed in Table 4, with the threshold 0.5. Our method achieves the best comprehensive performance over individual datasets and the merge of 4 datasets with different models.

Table 6: Evaluation results of different methods on various datasets using AUC, accuracy at corresponding threshold derived max G-Mean value (Acc). LLM-as-a-judge is the correctness measure. Same highlighting style as above.

Models	Datasets	TriviaQA + SQuAD	
	Methods	AUC	Acc
LLaMA-3.1-8B-Instruct	Perplexity	81.9	76.6
	Energy	79.7	71.8
	P(True)	82.5	74.1
	LNPE	83.1	76.2
	Semantic Entropy	78.6	69.6
	EigenScore	81.3	73.8
	AttnScore	54.4	50.6
	RePPL (Ours)	84.2	78.3
	SAPLMA*	84.9	76.6
	Probe-LR*	<u>86.1</u>	<u>78.1</u>
Probe-MM*	77.9	66.8	
Qwen-2.5-7B-Instruct	Perplexity	85.0	78.0
	Energy	85.4	78.7
	P(True)	85.6	80.3
	LNPE	85.5	79.5
	Semantic Entropy	81.5	78.8
	EigenScore	82.5	76.5
	AttnScore	68.2	62.5
	RePPL (Ours)	85.9	78.4
	SAPLMA*	<u>90.4</u>	<u>82.2</u>
	Probe-LR*	87.6	79.7
Probe-MM*	77.2	71.7	

F Comparision with Parameterized Probe-based Method

We present comparison results with parameterized probe methods in Table 4, Table 5, and Table 6. Our non-parameterized method is comparable to these strong methods. Given that these methods need extra engineering and are unable to work as uncertainty (hallucination risk) comparators without training, our non-parameterized method gains a good trade-off to be an effective uncertainty indicator with rich explainability.

G LLM-as-a-Judge-based Comparision

We also perform the experiment using LLM-as-a-judge as the correctness measure on the merge of the TriviaQA dataset and the SQuAD dataset. We apply DeepSeek-R1-250528 as the judge model to label whether the candidate responses from LLMs are hallucinated. The instruction for the judge model is demonstrated as follows:

Instruct: *You are tasked with evaluating whether a generated response is hallucinated compared to a reference answer. A hallucinated response includes factual inaccuracies or contradicts the reference (and the context in the user's question). Respond with "Yes" if the generated response contains hallucination. Respond with "No" if it is factually correct.*

Question: <Question>
Reference Answer: <Answer>
Generated Response: <Response>
Answer Yes or No:

We directly correspond ('Yes' and 'No') the output of DeepSeek-R1-0528 as the binary hallucination label. Since the PRR and Corr metrics are suitable for continuous scores between 0 to 1, we do not compute these two metrics with LLM-as-a-judge's 0-1 labels. Results are shown in Table 6, which demonstrates that our method is also effective.

H Runtime Analysis

We conduct a supplementary runtime analysis across four methods: EigenScore, AttnScore (LLM-Check), SAPLMA (trained probe), and our approach, on 100 randomly selected examples from TriviaQA and SQuAD using LLaMA-3.1-8B-Instruct. Each example involved 10 sampled outputs generated by the LLM. All methods are accounted for necessary forward passes, and inference is batched on 2 NVIDIA RTX 4090 GPUs (48GB total memory). The runtime results are summarized in Table 7.

Table 7: Runtime (in seconds, s) on 100 examples.

Method	TriviaQA	SQuAD
EigenScore	65.31s	165.07s
AttnScore	15.51s	32.34s
SAPLMA	15.55s	32.37s
RePPL (Ours)	74.37s	227.47s

As shown, our method maintains a runtime of approximately 2.3s per example, which is reasonable among sampling-based approaches. While slower than single-pass baselines, we argue the added explainability justifies the cost. In other words, we regard this trade-off as worthy since we bring better performance and explainability for hallucination detection.

I More Visual Explanations

We display 8 visual explanations on TriviaQA in Figure 8 and 4 visual explanations on SQuAD in Figure 9 (we mask the specific tokens for better presentation). As these figures show, distinctness between the hallucinated answers and the non-hallucinated answers is obvious. It also indicates that it is hard to detect hallucination with uncertainty in language generation alone.

J Details of Average Correlation

For Spearman Correlation computing, the significant value $p > 0.05$ ones are treated as 0 correlation, and when both the uncertainty score and importance score are masked as 0 at the same time for the same token, this pair is removed for correct computation.

<|begin_of_text|><|start_header_id|> **system**<|end_header_id|>
Cutting Knowledge Date: December 2023 Today Date: 26 Jul 2024
You are a helpful AI assistant. Answer user questions concisely, providing only the necessary information. Avoid full sentences.<|eot_id|><|start_header_id|> **user**<|end_header_id|>
The official birthday of British monarch Queen Elizabeth II falls during which month in the UK?<|eot_id|><|start_header_id|> **assistant**<|end_header_id|>
April<|eot_id|> **Hallucination**

<|begin_of_text|><|start_header_id|> **system**<|end_header_id|>
Cutting Knowledge Date: December 2023 Today Date: 26 Jul 2024
You are a helpful AI assistant. Answer user questions concisely, providing only the necessary information. Avoid full sentences.<|eot_id|><|start_header_id|> **user**<|end_header_id|>
Born 'Lucille LeSueur', By what name is this actress better known?<|eot_id|><|start_header_id|> **assistant**<|end_header_id|>
Greta Garbo.<|eot_id|> **Hallucination**

<|begin_of_text|><|start_header_id|> **system**<|end_header_id|>
Cutting Knowledge Date: December 2023 Today Date: 26 Jul 2024
You are a helpful AI assistant. Answer user questions concisely, providing only the necessary information. Avoid full sentences.<|eot_id|><|start_header_id|> **user**<|end_header_id|>
What letter is to the right of Q on a typewriter?<|eot_id|><|start_header_id|> **assistant**<|end_header_id|>
R<|eot_id|> **Hallucination**

<|begin_of_text|><|start_header_id|> **system**<|end_header_id|>
Cutting Knowledge Date: December 2023 Today Date: 26 Jul 2024
You are a helpful AI assistant. Answer user questions concisely, providing only the necessary information. Avoid full sentences.<|eot_id|><|start_header_id|> **user**<|end_header_id|>
Born 'Lucille LeSueur', By what name is this actress better known?<|eot_id|><|start_header_id|> **assistant**<|end_header_id|>
Greta Garbo.<|eot_id|> **Hallucination**

<|begin_of_text|><|start_header_id|> **system**<|end_header_id|>
Cutting Knowledge Date: December 2023 Today Date: 26 Jul 2024
You are a helpful AI assistant. Answer user questions concisely, providing only the necessary information. Avoid full sentences.<|eot_id|><|start_header_id|> **user**<|end_header_id|>
What was the capital of Poland prior to Warsaw?<|eot_id|><|start_header_id|> **assistant**<|end_header_id|>
Krakow.<|eot_id|> **No-Hallucination**

<|begin_of_text|><|start_header_id|> **system**<|end_header_id|>
Cutting Knowledge Date: December 2023 Today Date: 26 Jul 2024
You are a helpful AI assistant. Answer user questions concisely, providing only the necessary information. Avoid full sentences.<|eot_id|><|start_header_id|> **user**<|end_header_id|>
Who became the second Astronomer Royal upon the death of John Flamsteed in 1619?<|eot_id|><|start_header_id|> **assistant**<|end_header_id|>
Edmond Halley.<|eot_id|> **No-Hallucination**

<|begin_of_text|><|start_header_id|> **system**<|end_header_id|>
Cutting Knowledge Date: December 2023 Today Date: 26 Jul 2024
You are a helpful AI assistant. Answer user questions concisely, providing only the necessary information. Avoid full sentences.<|eot_id|><|start_header_id|> **user**<|end_header_id|>
What is normally celebrated on the third Sunday in June in the UK?<|eot_id|><|start_header_id|> **assistant**<|end_header_id|>
Father's Day.<|eot_id|> **No-Hallucination**

<|begin_of_text|><|start_header_id|> **system**<|end_header_id|>
Cutting Knowledge Date: December 2023 Today Date: 26 Jul 2024
You are a helpful AI assistant. Answer user questions concisely, providing only the necessary information. Avoid full sentences.<|eot_id|><|start_header_id|> **user**<|end_header_id|>
What criminal offence took place in Cheddington, Buckinghamshire in August (8th) 1963?<|eot_id|><|start_header_id|> **assistant**<|end_header_id|>
The Great Train Robbery.<|eot_id|> **No-Hallucination**

Figure 8: Visual explanations of the whole QA process on TriviaQA. The upper 4 are hallucinated ones, while the lower 4 are non-hallucinated ones.

<|begin_of_text|><|start_header_id|> **system**<|end_header_id|>
Cutting Knowledge Date: December 2023 Today Date: 26 Jul 2024
You are a helpful AI assistant. Answer user questions based on provided context concisely, providing only the necessary information. Avoid full sentences.<|eot_id|><|start_header_id|> **user**<|end_header_id|>
Context: Federal safety standards, such as NHTSA Federal Motor Vehicle Safety Standard 215 (pertaining to safety bumpers), and compacts like the 1974 Mustang I were a prelude to the DOT "downsize" revision of vehicle categories. By 1977, GM's full-sized cars reflected the crisis. By 1979, virtually all "full-size" American cars had shrunk, featuring smaller engines and smaller outside dimensions. Chrysler ended production of their full-sized luxury sedans at the end of the 1981 model year, moving instead to a full front-wheel drive lineup for 1982 (except for the M-body Dodge Diplomat/Plymouth Gran Fury and Chrysler New Yorker Fifth Avenue sedans). Question: Which car shows the DOT's revision of categories?<|eot_id|><|start_header_id|> **assistant**<|end_header_id|>
Chrysler New Yorker Fifth Avenue sedans.<|eot_id|> **Hallucination**

<|begin_of_text|><|start_header_id|> **system**<|end_header_id|>
Cutting Knowledge Date: December 2023 Today Date: 26 Jul 2024
You are a helpful AI assistant. Answer user questions based on provided context concisely, providing only the necessary information. Avoid full sentences.<|eot_id|><|start_header_id|> **user**<|end_header_id|>
Context: The connection between macroscopic nonconservative forces and microscopic conservative forces is described by detailed treatment with statistical mechanics. In macroscopic closed systems, nonconservative forces act to change the internal energies of the system, and are often associated with the transfer of heat. According to the Second law of thermodynamics, nonconservative forces necessarily result in energy transformations within closed systems from ordered to more random conditions as entropy increases. Question: What is the exchange of heat associated with?<|eot_id|><|start_header_id|> **assistant**<|end_header_id|>
Transfer of heat.<|eot_id|> **Hallucination**

<|begin_of_text|><|start_header_id|> **system**<|end_header_id|>
Cutting Knowledge Date: December 2023 Today Date: 26 Jul 2024
You are a helpful AI assistant. Answer user questions based on provided context concisely, providing only the necessary information. Avoid full sentences.<|eot_id|><|start_header_id|> **user**<|end_header_id|>
Context: Tymnet was an international data communications network headquartered in San Jose, CA that utilized virtual call packet switched technology and used X.25, SNA/SDLC, BSC and ASCII interfaces to connect host computers (servers) at thousands of large companies, educational institutions, and government agencies. Users typically connected via dial-up connections or dedicated async connections. The business consisted of a large public network that supported dial-up users and a private network business that allowed government agencies and large companies (mostly banks and airlines) to build their own dedicated networks. The private networks were often connected via gateways to the public network to reach locations not on the private network. Tymnet was also connected to dozens of other public networks in the U.S. and internationally via X.25/X.75 gateways. (Interesting note: Tymnet was not named after Mr. Tyme. Another employee suggested the name.) Question: How did user of Tymnet connect ?<|eot_id|><|start_header_id|> **assistant**<|end_header_id|>
Dial-up connections or dedicated async connection.<|eot_id|> **No-Hallucination**

<|begin_of_text|><|start_header_id|> **system**<|end_header_id|>
Cutting Knowledge Date: December 2023 Today Date: 26 Jul 2024
You are a helpful AI assistant. Answer user questions based on provided context concisely, providing only the necessary information. Avoid full sentences.<|eot_id|><|start_header_id|> **user**<|end_header_id|>
Context: Steam engines can be said to have been the moving force behind the Industrial Revolution and saw widespread commercial use driving machinery in factories, mills and mines; powering pumping stations; and propelling transport appliances such as railway locomotives, ships, steamboats and road vehicles. Their use in agriculture led to an increase in the land available for cultivation. There have at one time or another been steam-powered farm tractors, motorcycles (without much success) and even automobiles as the Stanley Steamer. Question: What is an example of a steam-powered automobile?<|eot_id|><|start_header_id|> **assistant**<|end_header_id|>
The Stanley Steamer.<|eot_id|> **No-Hallucination**

Figure 9: Visual explanations of the whole QA process on SQuAD. The Upper 2 are hallucinated ones, while the lower 2 are non-hallucinated ones.